Atmos. Chem. Phys. Discuss., doi:10.5194/acp-2016-808, 2016
Manuscript under review for journal Atmos. Chem. Phys.
Published: 5 October 2016

Atmospheric Chemistry and Physics Discussions

Upper Tropospheric Cloud Systems Derived from IR Sounders: Properties of Cirrus Anvils in the Tropics

Sofia E. Protopapadaki[1], Claudia J. Stubenrauch[1], and Artem G. Feofilov[1]

[1]Laboratoire de Météorologie Dynamique, IPSL/CNRS, UMR8539, Ecole Polytechnique, France

Correspondence to: S. Protopapadaki (sprotopap@lmd.polytechnique.fr)

Abstract. Representing about 30% of the Earth's total cloud cover, upper tropospheric clouds play a crucial role in the climate system by modulating the Earth's energy budget and heat transport. When originating from convection, they often form organized systems. The high spectral resolution of the Atmospheric InfraRed Sounder (AIRS) allows reliable cirrus identification, both from day and night-time observations. In this work, upper tropospheric cloud systems have been analysed by using a spatial composite technique on the retrieved cloud pressure of AIRS data. Convective core, cirrus, and thin cirrus anvil within these systems are distinguished by cloud emissivity. Combining AIRS cloud data with this cloud system approach, using physical variables, provides a new opportunity to relate the properties of the anvils, including also the thinner cirrus, to the convective cores. It also distinguishes convective cloud systems from isolated cirrus systems. A comparison with simultaneous precipitation data from the microwave sounder AMSR-E shows that large cloud emissivity is strongly correlated with rain rate, leading to a threshold of 0.98 in cloud emissivity to identify convective cores. Deep convective cloud systems, covering 15% of the tropics, are further distinguished into single-core and multi-core systems. Though AIRS samples the tropics only twice per day, we could show that, by using the fraction of convective core area within the cloud systems to stratify the properties of these systems, their life cycle can be statistically captured. This allows selecting mature convective cloud systems. For these systems, relationships between the physical properties of the anvils have been related to convective intensity. The latter has been identified by the minimum retrieved cloud temperature within the convective core. Our analyses show that the size of the systems do increase with convective intensity as expected. Furthermore, it was revealed that the fraction of thin cirrus over the total anvil area increases with increasing convective intensity, similarly for oceanic and continental convective systems.

1 Introduction

High clouds cover about 30% of the Earth (e.g Stubenrauch et al., 2013) and are of fundamental importance to climate as they modulate the Earth's energy budget and the heat transport in the upper troposphere, thus potentially influencing earth's atmospheric circulation and water cycle. Their feedbacks still lack of scientific understanding and heretofore represent a major uncertainty in predicting climate variability and climate change in climate models (Boucher et al., 2013).

In the tropics, where these clouds are most abundant, they often build large mesoscale systems of tens of thousands of km^2. They either form from organized deep convection or are directly formed *in situ*, when cold air is supersaturated with water. Within the last decade, numerous studies focused on these mesoscale convective cloud systems (MCS). Their structure and

Atmos. Chem. Phys. Discuss., doi:10.5194/acp-2016-808, 2016
Manuscript under review for journal Atmos. Chem. Phys.
Published: 5 October 2016

Atmospheric Chemistry and Physics Discussions

life cycle were studied by using composite techniques applied to satellite imagery and radar (e.g. Machado and Rossow, 1993; Machado et al., 1998; Del Genio and Kovari , 2002; Schumacher and Houze, 2003; Houze, 2004; Lin et al., 2006; Liu et al., 2007; Rossow et al., 2007; Yuan and Houze, 2010; Roca et al., 2014; Virts et al., 2015; Bouniol et al., 2016). These studies concentrated mainly on the thick cirrus anvils, because radar and visible-infrared imagery either miss or misidentify thin cirrus. The thinner cirrus are thought to be a part of the MCS's and have a significant radiative impact which might regulate convection itself (Stephens et al., 2004; Lebsock et al., 2010). Their radiative forcing depends primarily on their horizontal extent, emissivity distribution, and the temperature difference with the underlying surface.

In addition, organized convection was studied by statistical analysis of cloud regimes defined by similar cloud pressure and optical depth within grid cells (Tselioudis and Rossow, 2011; Rossow et al., 2013; Stachnik et al., 2013; Tan et al., 2015; Oreopoulos et al., 2016). Though this approach proved to be very useful for advancing our knowledge on tropical convection, it does not provide information of the horizontal extent and structure of the systems. Recent studies performed using the space-borne active instruments, lidar and radar, of the A-Train mission Stephens et al. (2002) revealed the vertical structure of these systems (e.g. Luo et al., 2010; Igel et al., 2014; Takahashi and Luo, 2014; Deng et al., 2016). They were, however, hampered by the very narrow track and thus are missing the horizontal extent of the system.

The good spectral resolution of infrared sounders, in particular the Atmospheric InfraRed Sounder (AIRS) aboard Aqua since 2002, and the Infrared Atmospheric Sounding Interferometers (IASI), aboard Metop since 2007, allows reliable cirrus identification, both from day and nighttime observations (e.g. Stubenrauch et al., 2010, 2013). Combining AIRS cloud data with a new cloud system approach, using physical cloud variables pressure and emissivity, provides a new opportunity to relate the properties of the anvils, including also the thinner cirrus, to the convective cores. This approach also distinguishes convective cloud systems from isolated cirrus systems. Details on the methodology are given in section 2. Results on the statistical properties of these tropical upper tropospheric cloud systems, their life-cycle, and the relationships between convective intensity and anvil properties are discussed in section 3. Conclusions are presented in section 4.

2 Methodology

2.1 Cloud properties derived from AIRS observations

The Atmospheric Infrared Sounder (AIRS) is an ultra-high spectral resolution infrared spectrometer, aboard the polar orbiting EOS Aqua satellite with an equatorial crossing at 1:30 a.m. and 1:30 p.m. local time (Chahine et al., 2006). AIRS completes approximately 14.5 orbits per day with each orbit 'swath' being of 48.95°, divided by 90 footprints for each scan line. The spatial resolution of a footprint varies from about 13.5 km x 21 km to 41 km x 21 km at the scan extremes. Level 2 cloud properties, such as emissivity, pressure, temperature and height have been produced over the whole globe and from 2003 to 2015 using the modular LMD CIRS methodology (Feofilov and Stubenrauch, 2016). It employs a weighted χ^2 method using eight channels along the CO_2 absorption band, from 11 to 14 micron and an a *posteriori* cloud detection based on the coherence of retrieved cloud emissivity between 10 and 12 micron (Stubenrauch et al., 2010, 2016). Cloud types are defined according to cloud pressure and cloud emissivity. Compared to the version which is distributed at the French data center ICARE and which

Atmos. Chem. Phys. Discuss., doi:10.5194/acp-2016-808, 2016
Manuscript under review for journal Atmos. Chem. Phys.
Published: 5 October 2016

Atmospheric Chemistry and Physics Discussions

has participated in the GEWEX cloud assessment (Stubenrauch et al., 2013), these cloud data are very similar for high-level clouds and with a detection slightly improved for low-level clouds (Stubenrauch et al., 2016).

To facilitate the reconstruction of the cloud systems from the L2 cloud properties, it is convenient to grid the data, keeping the statistics of the individual cloud types. The grid cell size should not be greater than the average size of the smallest cloud system. A good compromise was found by introducing grid cells of 0.5° in latitude and longitude.

2.2 Construction of Upper Tropospheric cloud systems

Before reconstructing the horizontal extent of the UT cloud systems, a critical question has to be addressed: how to define UT clouds? Most studies on tropical MCS's life cycle and structure, used the brightness temperature to define cold clouds. Yuan and Houze (2010) merge adjacent footprints containing cold clouds defined as those with T_B <260 K, while Machado et al. (1998) used T_B <245 K and, Fiolleau et al. (2013) and Roca et al. (2014) have considered only footprints with T_B <233 K. Brightness temperature depends on both cloud altitude and opacity; opaque clouds have a brightness temperature which indeed coincides with their actual temperature as shown in Fig. 1. However, for optically thinner clouds the radiation reaching the instrument includes in addition to the cloud's emission also a fraction of earth's surface and atmosphere radiation passing through them.

The present cloud system approach has the advantage of employing data in which the cloud altitude (temperature, pressure) and opacity (emissivity) are decoupled. Therefore, a clear distinction between high and low clouds is possible based on cloud pressure. Figure 1 presents the cloud brightness temperature as well as the retrieved cloud temperature as a function of the cloud emissivity for high clouds, with a pressure $<$ 440 hPa (corresponding to a height of about 7 km in the tropics). This definition of high clouds is generally found in the literature (e.g. Rossow et al., 1999; Stubenrauch et al., 2012). Indeed, T_B increases with decreasing cloud emissivity; an upper threshold on the T_B of 260 K will exclude from the analysis all high clouds with an emissivity below 0.6. As discussed in the introduction this new cloud system approach aims to understand the horizontal structure of the UT cloud systems, including thin cirrus.

Since the AIRS initial spatial resolution is more adapted to study organized convection rather than small scale shallow convection, we revise the definition of upper tropospheric clouds i) towards slightly higher clouds and ii) by using a tropopause dependent definition. Hereafter, UT clouds will be considered those being at most 250 hPa below the tropopause corresponding to a maximum cloud pressure of about 350 hPa and a height of about 8 km in the tropics. It should be stressed that the P$<$ 440 hPa high cloud definition has been also tested and the obtained results are compatible to these reported in section 3.

Typically, a convective system is composed of an opaque precipitating core which detrains cirrus in the form of an anvil at the height of neutral buoyancy (e.g. Luo et al., 2010; Takahashi and Luo, 2014). To investigate whether cloud emissivity can be used as a proxy to define the convective core, AIRS cloud data have been collocated with simultaneous AMSR-E precipitation data (Kummerow and Ferraro, 2006). Figure 2 presents the maximum and average rain rate from the AMSR-E measurements (of spatial resolution of about 5 km at nadir) within a grid cell as a function of cloud emissivity averaged from AIRS UT clouds within the same grid cell. Based on the previous plot, hereafter, convective cores are defined as those with ϵ_{cld} >0.98, since precipitation is significant, while cirrus and thin cirrus are defined by 0.98> ϵ_{cld} >0.5 and 0.5> ϵ_{cld} >0.1, respectively.

Atmos. Chem. Phys. Discuss., doi:10.5194/acp-2016-808, 2016
Manuscript under review for journal Atmos. Chem. Phys.
Published: 5 October 2016

Atmospheric Chemistry and Physics Discussions

To study the horizontal extent of cloud systems a full spatial coverage is required. However, in the tropical region ($30°N - 30°S$), AIRS measurements only cover about 70% due to gaps between orbits (e.g Fig.1 Feofilov et al., 2015). Thus, the missing data have to be extrapolated from the properties of the cloud types determined around the gaps. It should be stressed that days with missing orbits are completely excluded from the analysis; only scenes with coverage above 68%, representing more than 85% of the total statistics, are considered. In the following we describe the method developed to fill the missing data gaps. In each grid cell of 0.5°x0.5° the distribution of the number of measurements per cloud type is known. Cloud type distributions in empty grid cells are obtained from the probability density function (PDF) of the neighbouring grid cells. The PDF of an empty grid cell is built as the sum of the neighbouring PDFs, normalized to 1, weighted by the inverse squared root of the distance between the grid cells. Similarly, the physical properties of each cloud type in the interpolated grid, such as temperature, pressure and emissivity, are computed using the same weighted average method.

In the course of the study several questions emerged, such as how many neighbours to use, and what should be the shape of the region for the neighbors to be included in the interpolation. The reason we draw readers attention on these details is due to the irregular gap area shape and size which varies with latitude. The optimal filling configuration was deduced by statistically comparing the fractions of each of the UT cloud in the grid cells with real data and those with interpolated data, but also by visually examining geographical maps of cloud types such as Fig. 3 top panel. We found that the most appropriate way to get an UT cloud amount in the gaps consistent with the data grid cells, while preserving cloud system shapes, was to choose a number of neighbours proportional to the distance between the grid cells-to-be-filled and the closest non-empty-grid cell. By doing so, an empty grid cell surrounded by non-empty grid cells is filled using only a small number of the proximity data neighbours, while a cell located at the center of a gap near the equator (gap with maximum horizontal width) is filled using a larger number of data since the uncertainty is higher. The filling algorithm first scans eastward and westward of a grid cell to-be-filled to count the number of empty grid cells in both directions until a non-empty grid cell is found; the closest distance being the gap reference distance. Then, a spiral scan over the neighbours is performed for a number of cycles which increases linearly with the gap distance. From case studies we observed that obtaining realistic cloud system shapes requires the scan to be bound vertically to ± 3 grid cells, while allowing the horizontal scan free. As an example, top panel in Fig. 3 presents a geographic map of cloud types for one day in July at 1:30 AM LT, with the data gaps filed.

Once the gaps are filled, we apply a composite technique to reconstruct the upper tropospheric cloud systems; adjacent grid cells containing UT clouds and sharing a common side are grouped. The grid cells must contain more than 70% of UT cloud types within all AIRS measurements in order to be considered in the procedure. For interpolated grid cells the threshold is set slightly lower, to 65%, as this 5% difference corrects for an observed bias in the UT cloud amount of the interpolated areas. To ensure the spatial continuity of cloud systems, the average cloud pressure difference between two adjacent grid cells must be lower than 50 hPa; a legitimate value as it is slightly above the uncertainty of retrieved cloud pressure, which is of the order of 40 hPa (Stubenrauch et al., 2012; Feofilov and Stubenrauch, 2016) .

To identify opaque areas inside the built UT cloud systems, which potentially enclose convective core(s), a second grouping is performed. The emissivity limit for the opaque area definition is set to 0.9. The cloud system is then considered as "convective" when containing at least one grid cell with $\epsilon_{cld} > 0.98$ within the opaque area. The above core identification procedure

Atmos. Chem. Phys. Discuss., doi:10.5194/acp-2016-808, 2016
Manuscript under review for journal Atmos. Chem. Phys.
Published: 5 October 2016

Atmospheric Chemistry and Physics Discussions

provides the number of convective cores in a cloud system and thus allows its classification as non convective, if no convective core is found, or as convective if at least one core is found. The latter are further classified, with respect to the number of cores, to single-core and multi-core systems.

The bottom panel in Fig. 3 presents the UT cloud systems for the same day as in the top panel. Each cloud system has a different color, and the opaque and convective core areas are marked with magenta and deep red, respectively.

3 Results on Tropical Upper Tropospheric cloud systems

3.1 Statistical properties

We find that upper tropospheric cloud systems cover about 20% (25%) of the tropical band, defined as 30° N-30° S (15° N-15° S). Their horizontal extent varies significantly, starting from a single grid cell with a size of about 2500 km^2, reaching to several 10^8 km^2. These UT cloud systems may be distinguished as convective or non-convective (isolated cirrus) systems. More specifically, convective (single and multi-core) systems cover 15% (20%) while isolated cirrus systems cover 5% (5%) of the tropical band 30° N-30° S (15° N-15° S). The latter might originate from convection or formed by *in situ* freezing. Studies using Lagrangian transport performed by Luo et al. (2004) and Riihimaki et al. (2012) have shown that about 50% of these isolated cirrus systems form *in situ* while the other half corresponds to dissipating convective systems. Table 1 summarizes the statistical repartition of isolated cirrus systems, single-core and multi-core convective systems in the 30° N-30° S band along with their average sizes. As it can be seen, though isolated cirrus systems significantly outnumber the convective systems, their average horizontal extent is a factor of 10 smaller than the one of single-core convective systems. Multi-core convective systems are significantly larger than the other categories, compared to single-core by a factor of 20, while representing only 1% of the population. Among convective cloud systems, those having an horizontal extent larger than $3*10^8$ km^2 represent about 10% and are mainly located over the western Pacific during the monsoon period (Liu et al., 2007); a region with warm surface temperatures, large convective mass fluxes (Tissier et al., 2016), and large UT humidity (Virts et al., 2015; Houze et al., 2016). This region is also known for building mesoscale convective complexes (e.g. Mapes and Houze, 1993; Deng et al., 2016), including several convective systems, often in different phases of development and connected by ubiquitous thin cirrus.

Figure 4 presents the geographical distribution of a) isolated cirrus and b) all convective cores ($\epsilon_{cld} > 0.98$) of single and multi-core systems. The white areas contain less than five objects. The convective activity pattern clearly follows the Intertropical Convergence Zone (ITCZ) with maxima observed over the warm pool, north west south America and central Africa. The pattern is in agreement with previous findings obtained from the International Satellite Cloud Climatology Project (Tan et al., 2015), the CloudSat mission (Igel et al., 2014) and the Tropical Rainfall Measuring Mission (Houze et al., 2015). As expected, isolated cirrus are abundant and are found to cover much wider areas in the vicinity of the convective active regions.

Atmos. Chem. Phys. Discuss., doi:10.5194/acp-2016-808, 2016
Manuscript under review for journal Atmos. Chem. Phys.
Published: 5 October 2016

Atmospheric Chemistry and Physics Discussions

3.2 System composition and life-cycle stages

As discussed in the introduction, the impact of UT cloud systems on the Earth's energy budget depends on their horizontal extent, their emissivity distribution, and the temperature difference between the cloud and its underlying surface (lower clouds or earth surface). The latter has been explored by Haladay and Stephens (2009). In this work, the first two points will be studied.

Hereafter, as we have enough statistics and as we are primarily interested on studying individual cloud systems structure, rather than on the total coverage of the tropical band, to keep the uncertainties low, only convective cloud systems which are composed with more than 80% of data will be considered in the analyses.

Figure 5 presents the average proportion of convective core, thick and thin anvils as a function of the UT cloud system horizontal extent, separately for single and multi-core convective systems. The statistics includes convective systems at different phases of their life cycle (in development and mature). As the systems get larger, the fraction of the convective core decreases to 10% and that of thin cirrus anvil increases up to about 30%. The same tendencies are observed for both single and multi-core systems, with the only difference that the latter have slightly smaller fractions of convective core area and slightly larger fractions of thin cirrus area.

The composition of a convective system (convective part, thick and thin anvil) depends on the system life-cycle stage. With increasing size, the life-cycle of these systems varies from a couple of hours up to several days, as shown by Machado et al. (1998) and Fiolleau et al. (2013), with the maximum horizontal extent of the thicker anvil attained at the mature stage (Machado and Rossow, 1993; Futyan and Del Genio, 2007; Takahashi and Luo, 2014).

In this analysis, using snapshots which are available only every twelve hours, the life cycles of the convective systems cannot be directly tracked. Nevertheless, we will use the fraction of the convective area, as defined in section 2.2, to get an indirect insight on the life cycle stage of convective systems.

Figure 6 shows the normalized distribution of convective core fraction, separately for single and multi-core systems. In general, this fraction has a wider distribution and peaks at a larger value for single-core systems compared to multi-core convective systems (at 0.25 and 0.1, respectively). A small fraction of single-core convective systems consist only of the convective core; these are systems probably in the development phase. Only during maturity and dissipation convective systems include increasing upper tropospheric stratiform cirrus anvils, while the fraction of the convective area decreases (e.g Leary and Houze, 1979; Machado and Rossow, 1993). Multi-core convective systems, agglomerating convective systems probably in different stages of development, are not suitable for exploring the system's life cycle, and therefore will not be considered in this study.

By stratifying the physical properties of the single-core convective systems according to their fraction of convective area within the cloud system, we explore whether they follow an evolution pattern which corresponds to different life cycle stages. To do so, we consider eleven intervals of equal statistics with respect to the convective fraction: [1, 0.78, 0.65, 0.55, 0.47, 0.40, 0.34, 0.29, 0.24, 0.19, 0.13, 0.01]. Figure 7 presents the physical properties of single-core convective systems for successive life cycle stages, separately in the early afternoon (PM) and at night (AM), over land and over ocean. While the total cloud system horizontal extent (Fig. 7 a) increases during the whole life cycle stage with a maximum at the dissipating stage (convective

Atmos. Chem. Phys. Discuss., doi:10.5194/acp-2016-808, 2016
Manuscript under review for journal Atmos. Chem. Phys.
Published: 5 October 2016

Atmospheric Chemistry and Physics Discussions

fraction lower than 10%), the horizontal extent of the convective core (Fig. 7b) increases until it reaches a plateau around life cycle stage 5-9, which corresponds to a convective fraction between about 0.1 and 0.3. The behaviour is similar over land and ocean, except for ocean in the early afternoon, where the increase in convective core size is stronger with a peak for cloud systems with a convective fractional area of about 0.2. Compared to earlier studies using brightness temperature to define cold clouds (e.g. Machado and Rossow, 1993), these figures show that it is the thicker part of the cloud system which increases in size while reaching maturity and then decreases towards dissipation, whereas including the thin cirrus anvil leads to a continuous increase until dissipation. When considering the evolution of the emissivity distribution within the convective system (Fig. 7c) and the ratio of thin cirrus over cirrus within the anvil (Fig. 7d), the average emissivity of the cloud system decreases and moreover the fraction of thin anvil increases along the system's life cycle in agreement with expectations. It is interesting to note that the behaviour is similar over ocean and over land. Rain rate is maximum at the developing phase and decreases successively until dissipation (Fig. 7e), with twice higher rates over land than over ocean. The minimum temperature of the convective core is the only variable which has not a clear behaviour for all scenes: only over land we observe a decrease in temperature, corresponding to an increase in height, during the phase of development, with colder temperatures in the afternoon than during night. Over ocean the temperature of the systems is constant and colder during night whereas during day the temperature decreases slowly until dissipation. All minimum temperatures are similar for dissipating convective systems. Considering the statistics of the cloud systems for the different 'life cycle stages' in Fig. 8, one observes that in the early afternoon convective systems over ocean are mostly in the dissipating phase whereas those over land are more in the developing stage. During night the statistics is more equally distributed, with twice as many oceanic single-core convective systems than in the afternoon. These findings are in agreement with studies on tropical precipitation which show a peak in the late afternoon over land and a few hours before sunrise over ocean (e.g. Liu et al., 2007).

3.3 Relationships between convective intensity and cirrus anvil properties

The horizontal extent of the UT cloud systems directly impacts the Earth's energy budget. Since we are interested on how the properties of the cirrus anvils are related to convection itself, we have first to find proxies for convective intensity. Previous studies used as a convective intensity indicator the precipitation area (Yuan and Houze, 2010), or the width of the convective tower (Igel et al., 2015), or the radar signal (Liu et al., 2007; Takahashi and Luo, 2014), or brightness temperature (Machado et al., 1998; Jiang , 2012). While cloud emissivity is a good indicator for the convective core definition (Fig. 2), it saturates at 1 and thus can not be used as a proxy for convective intensity. However, as one can see in Fig. 7, the fraction of convective core area might be used as a proxy for the maturity stage. In the following, we will investigate convective intensity only for mature convective systems which are defined from Fig. 7 as systems for which the fraction of convective core area varies between 0.1 and 0.3.

A proxy for convective intensity might be the height of the convective system which is indicated by the temperature of the convective core. On the other hand, by defining the convective core by $\epsilon_{cld} > 0.98$, it might also include parts of the rainy anvil. Therefore, a better proxy for convective intensity should be the minimum temperature within the convective core (T^{cb}_{min}). A

Atmos. Chem. Phys. Discuss., doi:10.5194/acp-2016-808, 2016
Manuscript under review for journal Atmos. Chem. Phys.
Published: 5 October 2016

Atmospheric Chemistry and Physics Discussions

similar variable, the minimum brightness temperature within the convective core, has been shown to be a more skillful proxy to describe convective intensity, compared to the echo radar height (Jiang , 2012).

To test this hypothesis, we consider in Fig. 9 the relation between T_{min}^{cb} and the average rain rate within the convective core, separately over land and ocean; all convective cores are included, both of single and multi-core convective systems. From Fig. 9 we deduce that the colder (higher) the convective core, the higher is its rain rate, indicating that the minimum temperature within the convective core is indeed a good proxy for convective strength or intensity. The relationship is similar over ocean and over land, with the difference that the average rain rate is higher over land than over ocean for the same coldest core temperature. This can be explained by stronger convective activity over land and by a rain detection offset over land. This suggests that our proxy is a good qualitative indicator of convective intensity, but for the same T_{min}^{cb}, strongly related to the height of the convective tower, the oceanic convective cores produce less rain than the continental convective cores.

Figure 10 presents the size of the mature convective systems as a function of the minimum temperature within the convective core, separately for oceanic and for continental systems. We observe an increase of the size of the systems with increasing convective intensity, represented by decreasing T_{min}^{cb}. This is in agreement with the expectation that more intense convection will lead to larger anvils (e.g. Igel et al., 2014, 2015). Whereas it is straightforward to determine the minimum temperature within a single-core convective system, it is more difficult to consider this proxy for multi-core convective systems. The latter might be composed of several convective sub-systems in different phases of development. Nevertheless, we build for those systems the average T_{min}^{cb} over all convective cores of the system. Considering Fig. 11, one observes that multi-core convective systems behavior is analogous to single-core systems. From Fig. 9, 10 and 11 we conclude that for both single and multi-core systems, oceanic convective systems of a similar convective intensity as continental systems have a larger size with less intense convective rain. This difference in structure was already pointed out in earlier studies (e.g. Liu et al., 2007).

The next question is: will there also be a difference in the anvil horizontal structure with increasing convective intensity?

Figure 12 shows the ratio of thin cirrus anvil area over total anvil size as a function of T_{min}^{cb} for single-core convective systems, separately over land and over ocean. With increasing convective intensity (decreasing T_{min}^{cb}) the fraction of thin cirrus anvil increases, and this in the same manner for oceanic convective systems as for continental systems. Figure 13 presents the same quantities, this time land and oceanic systems are merged, separately for single and multi-core systems. We also observe a very similar behavior for single-core convective systems and multi-core systems. These results indicate a clear relationship between convective intensity and the properties of the detrained cirrus anvils. To go one step further in our investigation, Fig. 14 shows how the cirrus anvil emissivity varies with increasing distance to the convective core, normalized by dividing with the square root of the size, for single-core systems. Three intervals of T_{min}^{cb} are considered, representing systems with different convective intensity. For all systems the cirrus anvil emissivity decreases with increasing distance, as one would expect. While the decrease in emissivity is comparable for all systems within the first quarter of the horizontal extent, is continues to decrease more rapidly for systems with strong convective intensity compared to those originating from less intense convection. This might have important implications for the radiative impact of these systems in relation to increasing convective intensity in a warming climate.

Atmos. Chem. Phys. Discuss., doi:10.5194/acp-2016-808, 2016
Manuscript under review for journal Atmos. Chem. Phys.
Published: 5 October 2016

Atmospheric Chemistry and Physics Discussions

4 Conclusions

We have build UT cloud systems from InfraRed Sounder cloud data. 13 years AIRS cloud climate data, retrieved at LMD, have been used to investigate the relations between the convective intensity of tropical mesoscale convective systems and the properties of the surrounding cirrus anvils.

The benefits of the present cloud system approach compared to other studies, are that 1) IR sounder data have a large instantaneous coverage and are sensitive to thin cirrus down to an emissivity of 0.1 (0.2 in visible optical depth) and 2) the cloud retrieval provides the physical properties to reconstruct the horizontal extent of the UT cloud systems and to distinguish between isolated cirrus and deep convective systems. For the latter, the cloud emissivity permits to differentiate convective cores, cirrus and thin cirrus anvils as well as to identify single-core and multi-core convective systems. UT cloud systems cover about 20%-25% of the tropics. While the frequency strongly decreases from isolated cirrus towards multi-core convective systems, the latter's coverage is the largest.

By using the fractional area of the convective core as a proxy for the stage of the cloud system development, the properties of single-core convective systems could be statistically followed during their life-cycle. We observed that with decreasing convective core fraction, which means moving towards maturity and dissipation, the rain rate within the convective core decreases while the horizontal extent and emissivity of the UT cloud systems decrease, as expected. The size of the convective core reaches a plateau and then decreases during the stage of dissipation, guiding us to define mature convective systems as those with a convective core fraction between 0.1 and 0.3. Convective intensity has then been studied for mature convective systems, and it could be shown that the minimum temperature within the convective core is a good proxy. Colder convective systems (meaning also rising higher) have a larger rain rate within the convective core and lead to larger cirrus anvils, in agreement with earlier studies. Since our approach also allows to study the emissivity structure within the anvils, we investigated it in relation with convective intensity. It was revealed that the fraction of thin cirrus over the total anvil area increases with increasing convective intensity, similarly for oceanic and continental convective systems and both for single and multi-core systems. We also demonstrated that with increasing convective intensity of the system the emissivity of the anvil decreases in general more sharply with increasing distance to the convective core. This might have important implications for the radiative effects of these systems, in relation to a convection intensity increase in a warming climate.

The above findings are very promising. As a future perspective, the developed cloud system approach could be the basis to address the question of what are UT cloud feedbacks in modulation atmospheric circulation and how they will evolve with climate change. To do so, the main components which have to be added to the presented dataset are the vertical structure of the cloud systems and information on their atmospheric environment. Furthermore, Lagrangian transport analysis could be used to indicate the origin of the isolated cirrus systems and to assess the link between convective sources and the air entering the stratosphere. This new cloud system approach can also be used to evaluate cloud resolving models and climate models and to constrain parameterizations related to convection and anvil detainment processes by examining relationships as those presented here.

Atmos. Chem. Phys. Discuss., doi:10.5194/acp-2016-808, 2016
Manuscript under review for journal Atmos. Chem. Phys.
Published: 5 October 2016

Acknowledgements. This research was supported by the Centre National d'Etudes Spatiales (CNES), the Centre National de la Recherche Scientifique (CNRS) and the European Space Agency (ESA), within its framework of ESA Climate Change Initiative. The authors also thank the Earth Observing System AIRS and AMSR-E teams for providing the data. The calculations have been performed at the ClimServ IPSL centre.

Atmos. Chem. Phys. Discuss., doi:10.5194/acp-2016-808, 2016
Manuscript under review for journal Atmos. Chem. Phys.
Published: 5 October 2016

Atmospheric Chemistry and Physics Discussions

References

Boucher, O., D. Randall, P. Artaxo, C. Bretherton, G. Feingold, P. Forster, V.-M. Kerminen, Y. Kondo, H. Liao, U. Lohmann, P. Rasch, S.K. Satheesh, S. Sherwood, B. Stevens, and X.Y. Zhang, Clouds and aerosols. In Climate Change 2013: The Physical Science Basis. Contribution of Working Group I to the Fifth Assessment Report of the Intergovernmental Panel on Climate Change. T.F. Stocker, D. Qin, G.-K. Plattner, M. Tignor, S.K. Allen, J. Doschung, A. Nauels, Y. Xia, V. Bex, and P.M. Midgley, Eds. Cambridge University Press, 571-657, 2013.

Bouniol, D., R. Roca, Thomas Fiolleau, and D. Emmanuel Poan, Macrophysical, Microphysical, and Radiative Properties of Tropical Mesoscale Convective Systems over Their Life Cycle., J.Climate, 29, 3353-3371, 2016.

Moustafa T. Chahine, Thomas S. Pagano, Hartmut H. Aumann, Robert Atlas, Christopher Barnet, John Blaisdell, Luke Chen, Murty Divakarla, Eric J. Fetzer, Mitch Goldberg, Catherine Gautier, Stephanie Granger, Scott Hannon, Fredrick W. Irion, Ramesh Kakar, Eugenia Kalnay, Bjorn H. Lambrigtsen, Sung-Yung Lee, John Le Marshall, W. Wallace McMillan, Larry McMillin, Edward T. Olsen, Henry Revercomb, Philip Rosenkranz, William L. Smith, David Staelin, L. Larrabee Strow, Joel Susskind, David Tobin, Walter Wolf, and Lihang Zhou, AIRS: Improving Weather Forecasting and Providing New Data on Greenhouse Gases., Bull. Amer. Meteor. Soc., 87, 911-926, 2006.

Del Genio, A.D., and W. Kovari, Climatic properties of tropical precipitating convection under varying environmental conditions., J. Climate, 15, 2597-2615, 2002.

Deng Q, Khouider B, Majda AJ, Ajayamohan RS, Effect of stratiform heating on the planetary-scale organization of tropical convection., J Atmos Sci 73:371-392, 2016.

Feofilov, A. G., C. J. Stubenrauch, and J. Delanoë, Ice water content vertical profiles of high-level clouds: classification and impact on radiative fluxes,Atmos. Chem. Phys., 15, 12327-12344, 2015.

Feofilov, A. and Stubenrauch, C., LMD Cloud Retrieval using IR sounders: Algorithm Theoretical Basis Document, CIRS-LMD software package V2 19 pp., available at LMD, 2016.

Fiolleau, T. and Roca, R., Composite life cycle of tropical mesoscale convective systems from geostationary and low Earth orbit satellite observations: method and sampling considerations, Q.J.R. Meteorol. Soc., 139: 941-953, 2013.

Futyan, J., and A. Del Genio, Deep convective system evolution over Africa and the tropical Atlantic, J. Climate, 20, 5041-5060, 2007.

Haladay T, Stephens G., Characteristics of tropical thin cirrus clouds deduced from joint CloudSat and CALIPSO observations, Journal of Geophysical Research, 114, 2009.

Houze, Robert A., Mesoscale convective systems, Reviews of Geophysics, 42 ,4 , 1944-9208, 2004.

Houze, Robert A. and Rasmussen, Kristen L. and Zuluaga, Manuel D. and Brodzik, Stella R., The variable nature of convection in the tropics and subtropics: A legacy of 16 years of the Tropical Rainfall Measuring Mission satellite, Reviews of Geophysics,53,3,3,1944-9208, 2015.

Houze, R. A. Jr., K. L. Rasmussen, L. McMurdie, M. M. Chaplin, and A. Kumar, Synoptic and mesoscale aspects of the June 2013 flooding in Uttarakhand, India, Quart. J. Roy. Meteor. Soc., submitted, 2016.

Matthew R Igel and Aryeh J Drager and Susan C Van Den Heever, A CloudSat cloud object partitioning technique and assessment and integration of deep convective anvil sensitivities to sea surface temperature, Journal of Geophysical Research: Atmospheres, 119, 17,2169-8996, 2014.

Igel, M. R. and van den Heever, S. C., Tropical, oceanic, deep convective cloud morphology as observed by CloudSat, Atmos. Chem. Phys. Discuss., 15, 2015.

Atmos. Chem. Phys. Discuss., doi:10.5194/acp-2016-808, 2016
Manuscript under review for journal Atmos. Chem. Phys.
Published: 5 October 2016

Jiang Haiyan, The Relationship between Tropical Cyclone Intensity Change and the Strength of Inner-Core Convection, Monthly Weather Review, 140, 4, 1164-1176, 2012.

Kummerow, C., and R. Ferraro, EOS/AMSR-E Level-2 Rainfall: Algorithm Theoretical Basis Document, Fort Collins, Colorado, USA: Colorado State University,(PDF file, 245 KB)http://nsidc.org/sites/nsidc.org/files/files/amsr_atbd_supp06_L2_rain.pdf, 2006.

Leary, C. A., and R. A. Houze, Jr., Melting and evaporation of hydrometeors in precipitation from the anvil clouds of deep tropical convection, J. Atmos. Sci., 36, 669-679, 1979.

Matthew D. Lebsock and Christian Kummerow and Graeme L. Stephens, An Observed Tropical Oceanic Radiative¿Convective Cloud Feedback, Journal of Climate, 23, 8, 2065-2078, 2010.

Lin, J.-L., G.N. Kiladis, B.E. Mapes, K.M. Weickmann, K.R. Sperber, W. Lin, M.C. Wheeler, S.D. Schubert, A. Del Genio, L.J. Donner, S. Emori, J.-F. Gueremy, F. Hourdin, P.J. Rasch, E. Roeckner, and J.F. Scinocca, Tropical intraseasonal variability in 14 IPCC AR4 climate models. Part I: Convective signals, J. Climate, 19, 2665-2690, 2006.

Liu, C., E. J. Zipser, and S. W. Nesbitt, Global Distribution of Tropical Deep Convection: Different Perspectives from TRMM Infrared and Radar Data, J. Climate, 20, 489-503, 2007.

Luo Z. and Rossow W. B., Characterizing Tropical Cirrus Life Cycle, Evolution, and Interaction with Upper-Tropospheric Water Vapor Using Lagrangian Trajectory Analysis of Satellite Observations, J. Climate, 17, 4541-4563, 2004.

Luo, Z. J. , G. Y. Liu, and G. L. Stephens, Use of A-Train data to estimate convective buoyancy and entrainment rate, Geophys. Res. Lett. 37, L09804, 2010.

Machado, L. A. T. and Rossow, W. B., Structural characteristics and radiative properties of tropical cloud clusters, Mon. Wea. Rev., 121, 3234-3260., 1993.

Machado, L.A.T., W.B. Rossow, R.L. Guedes, and A.W. Walker, Life cycle variations of mesoscale convective systems over the Americas, Mon. Weather Rev., 126, 1630-1654, 1998.

Mapes, B. E., and R. A. Houze, Jr., Cloud clusters and superclusters over the oceanic warm pool, Mon. Wea. Rev., 121, 1398-1415, 1993.

Oreopoulos, L., N. Cho, D. Lee, and S. Kato, Radiative effects of global MODIS cloud regimes, J. Geophys. Res., 121, 2299-2317, 2016.

Roca, R., J. Aublanc, P. Chambon, T. Fiolleau, and N. Viltard, Robust Observational Quantification of the Contribution of Mesoscale Convective Systems to Rainfall in the Tropics, J. Climate, 27, 4952-4958, 2014.

William B. Rossow and Robert A. Schiffer, Advances in Understanding Clouds from ISCCP, Bulletin of the American Meteorological Society, 80,11,2261-2287, 1999.

Rossow, W.B., and C. Pearl, 22-yr survey of tropical convection penetrating into the lower stratosphere, Geophys. Res. Lett., 34, L04803, 2007.

Rossow, W. B., A. Mekonnen, C. Pearl, and W. Goncalves, Tropical Precipitation Extremes,J. Climate, 26, 1457-1466, 2013.

Schumacher, C., and R. A. Houze, Jr., Stratiform rain in the tropics as seen by the TRMM Precipitation Radar, J. Climate, 16, 1739-1756, 2003.

Stachnik, J. P., C. Schumacher, and P. E. Ciesielski, Total Heating Characteristics of the ISCCP Tropical and Subtropical Cloud Regimes, J. Climate, 26, 7097-7116, 2013.

Stephens, G.L., D.G. Vane, R.J. Boain, G.G. Mace, K. Sassen, Z. Wang, A.J. Illingworth, E.J. O'Connor, W.B. Rossow, S.L. Durden, S.D. Miller, R.T. Austin, A. Benedetti, C. Mitrescu, and CloudSat Science Team, The CloudSat mission and the A-Train: A new dimension of space-based observations of clouds and precipitation, Bull. Amer. Meteorol. Soc., 83, 1771-1790, 2002.

Stephens, G. L., P. J. Webster, R. H. Johnson, R. Engelen, and T. L'Ecuyer, Observational Evidence for the Mutual Regulation of the Tropical Hydrological Cycle and Tropical Sea Surface Temperatures, J. Climate 17, 2213-2224, 2004.

Stephens, G. L. and Ellis, T. D., Controls of Global-Mean Precipitation Increases in Global Warming GCM Experiments, Journal of Climate,21,23,6141-6155, 2008.

Stubenrauch, C. J., A. Chédin, R. Armante, and N. A. Scott, Clouds as seen by Infrared Sounders (3I) and Imagers (ISCCP): Part I Evaluation of Cloud Parameters, J. Climate, 12, 2189-2213, 1999.

Stubenrauch C. J.. S. Cros. A. Guignard, and N. Lamquin, A six-year global cloud climatology from the Atmospheric InfraRed Sounder aboard the Aqua Satellite: statistical analysis in synergy with CALIPSO and CloudSat, Atmos. Chem. Phys., 10, 7197-7214, 2010.

Stubenrauch, C. J., W. B. Rossow, and S. Kinne, Assessment of global cloud datasets from satellites: A project of the World Climate Research Programme Global Energy and Water Cycle Experiment (GEWEX) Radiation Panel, WCRP Rep. 23/2012, 176 pp., 2012.

Stubenrauch, C. J. and W. B. Rossow and S. Kinne and S. Ackerman and G. Cesana and H. Chepfer and L. Di Girolamo and B. Getzewich and A. Guignard and A. Heidinger and B. C. Maddux and W. P. Menzel and P. Minnis and C. Pearl and S. Platnick and C. Poulsen and J. Riedi and S. Sun-Mack and A. Walther and D. Winker and S. Zeng and G. Zhao, Assessment of Global Cloud Datasets from Satellites: Project and Database Initiated by the GEWEX Radiation Panel, Bulletin of the American Meteorological Society, 94, 7, 1031-1049, 2013.

Stubenrauch, C. J., A. G. Feofilov, S. Protopapadaki, and R. Armante, Cloud climatologies from InfraRed Sounders (AIRS and IASI) using the LMD cloud retrieval: sensitivity studies, statistical analysis and vertical structure in synergy with CALIPSO and CloudSat, to be submitted to Atmos. Chem. Phys. Discuss, 2016.

Riihimaki, Laura D. and McFarlane, Sally A. and Liang, Calvin and Massie, Steven T. and Beagley, Nathaniel and Toth, Travis D., Comparison of methods to determine Tropical Tropopause Layer cirrus formation mechanisms, Journal of Geophysical Research: Atmospheres, 117,D6,2156-2202, 2012.

Takahashi, H., and Z. Luo, Where is the level of neutral buoyancy for deep convection?, Geophys. Res. Lett., 39, L15809, 2012.

Takahashi, H. and Z. J. Luo, Characterizing Tropical Overshooting Convection from Joint Analysis of CloudSat and Geostationary Satellite Observations.,J. Geophys. Res., 119, 112-121, 2014.

Tan, J., C. Jakob, W.B. Rossow, and G. Tselioudis, Increases in tropical rainfall driven by changes in frequency of organized deep convection, Nature, 519, 451-454, 2015.

Tissier, A.-S. and Legras, B., Convective sources of trajectories traversing the tropical tropopause layer, Atmospheric Chemistry and Physics,16,5,3383-3398, 2016.

Tselioudis, G., and W.B. Rossow, Time scales of variability of the tropical atmosphere derived from cloud-defined weather states, J. Climate, 24, 602-608, 2011.

Virts, K. S., and R. A. Houze Jr, Clouds and Water Vapor in the Tropical Tropopause Transition Layer over Mesoscale Convective Systems, J. Atmos. Sci., 72, 4739-4753, 2015.

Yuan, J., and R. A. Houze, Jr., Global variability of mesoscale convective system anvil structure from A-train satellite data, J. Climate, 23, 5864-5888, 2010.

Atmos. Chem. Phys. Discuss., doi:10.5194/acp-2016-808, 2016
Manuscript under review for journal Atmos. Chem. Phys.
Published: 5 October 2016

Atmospheric Chemistry and Physics Discussions

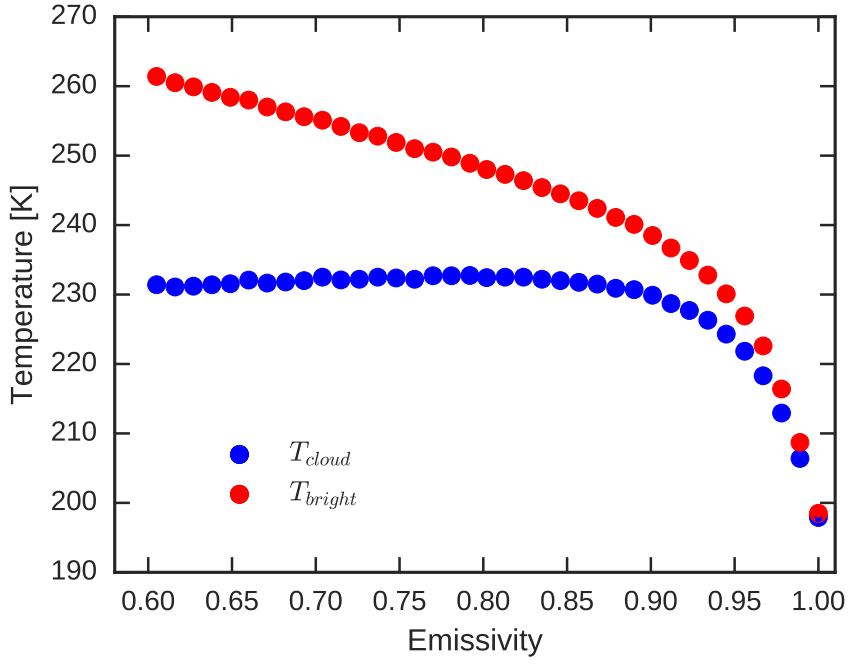

Figure 1. Cloud brightness temperature (red) and retrieved cloud temperature (blue) as a function of cloud emissivity for high clouds identified from AIRS observations, at a spatial resolution of 0.5°.

Atmos. Chem. Phys. Discuss., doi:10.5194/acp-2016-808, 2016
Manuscript under review for journal Atmos. Chem. Phys.
Published: 5 October 2016

Atmospheric Chemistry and Physics Discussions

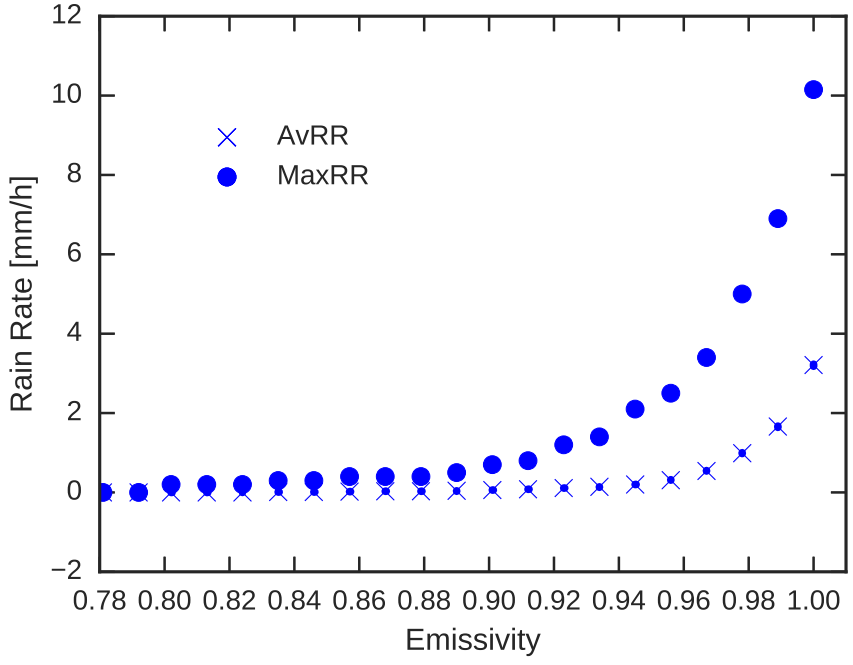

Figure 2. Maximum (circle) and average (x) rain rate from AMSR-E as a function of cloud emissivity for AIRS high clouds, at a spatial resolution of 0.5°.

Atmos. Chem. Phys. Discuss., doi:10.5194/acp-2016-808, 2016
Manuscript under review for journal Atmos. Chem. Phys.
Published: 5 October 2016

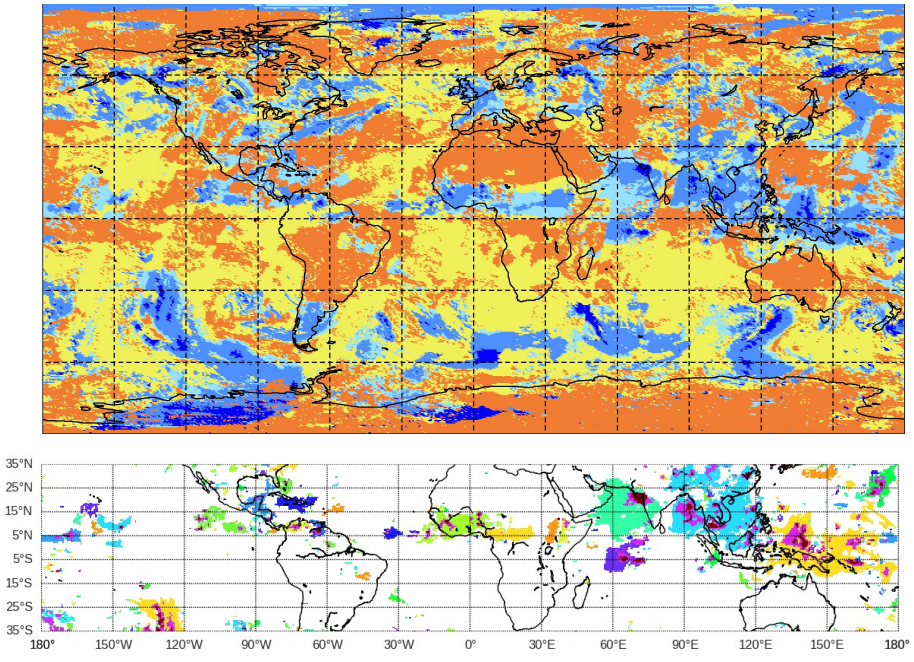

Figure 3. Geographic map of AIRS cloud data for 1 July 2007, 1:30 h local time. Top: cloud types, with blue → upper tropospheric clouds (more opaque deeper blue), yellow → midlevel and low clouds and orange → clear sky. Bottom: UT cloud systems, the different colors indicate different systems, opaque and convective areas marked with magenta and deep red, respectively.

Atmos. Chem. Phys. Discuss., doi:10.5194/acp-2016-808, 2016
Manuscript under review for journal Atmos. Chem. Phys.
Published: 5 October 2016

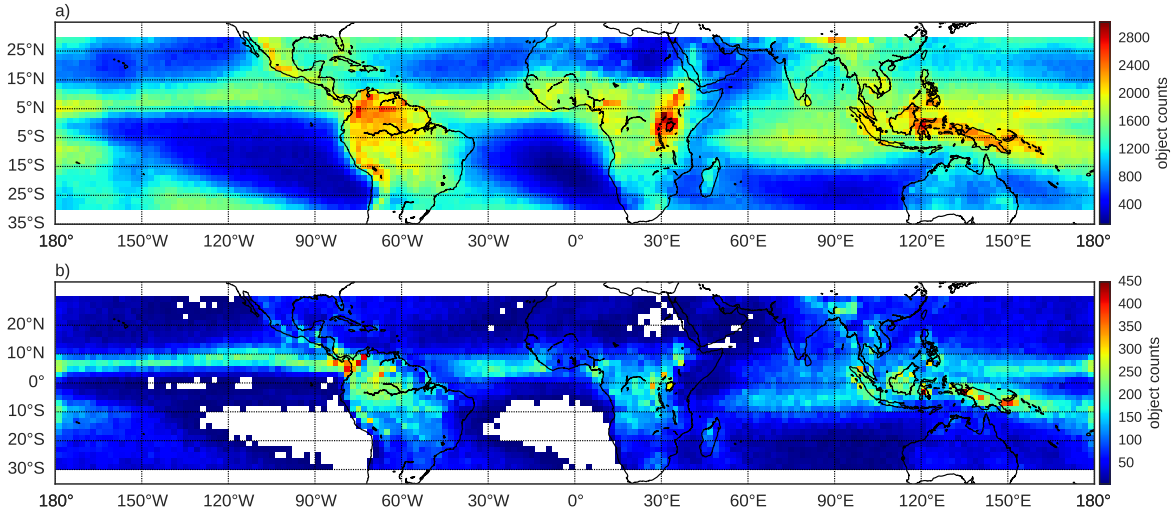

Figure 4. Geographic maps of isolated cirrus systems (top) and convective cores (bottom), for the 2003-2015 period of the LMD AIRS cloud climatology.

Atmos. Chem. Phys. Discuss., doi:10.5194/acp-2016-808, 2016
Manuscript under review for journal Atmos. Chem. Phys.
Published: 5 October 2016

Atmospheric Chemistry and Physics Discussions

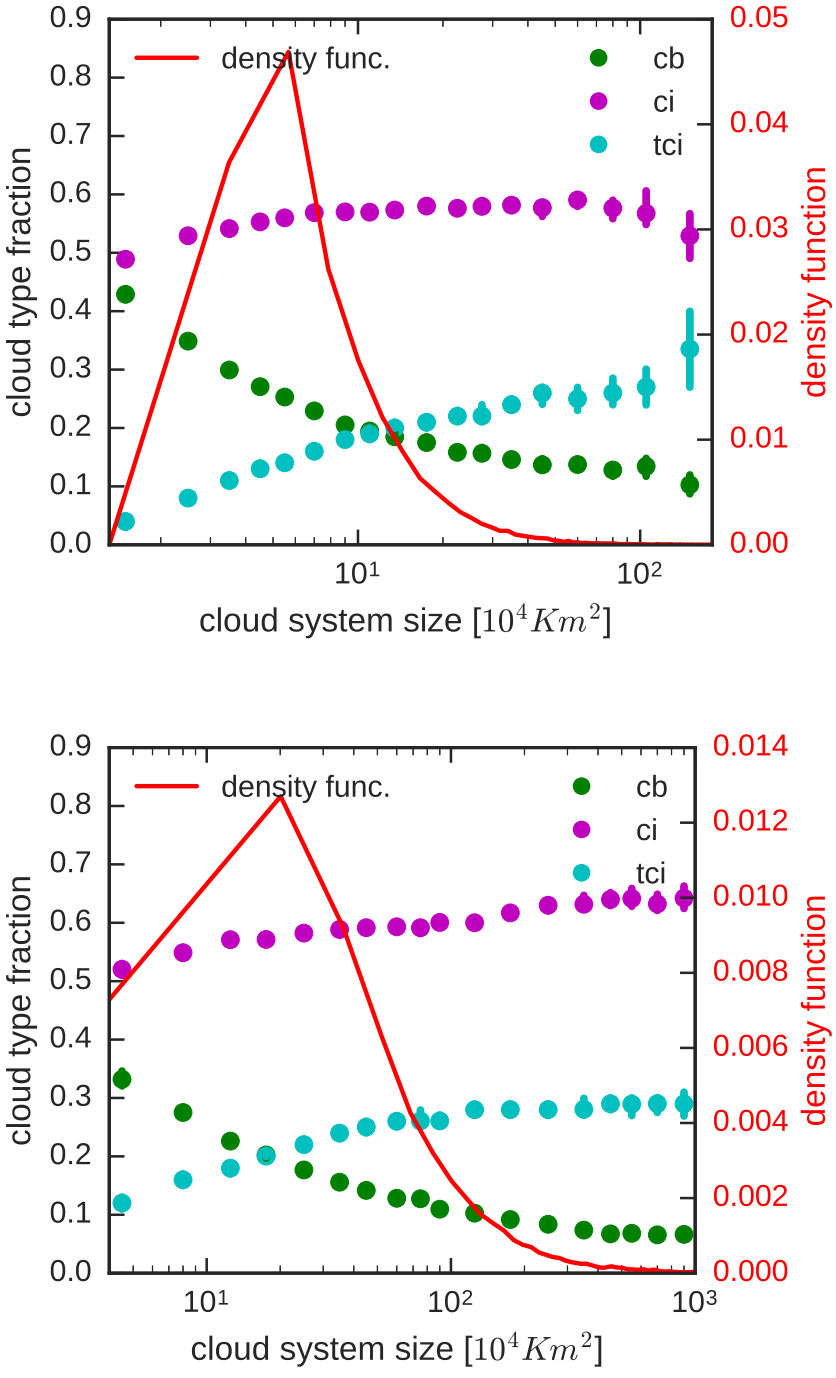

Figure 5. Fraction of convective core (green), thick (magenta) and thin (cyan) anvil as a function of cloud system size. In red, cloud system size density function distribution. Top: single-core, bottom: multi-core systems.

Atmos. Chem. Phys. Discuss., doi:10.5194/acp-2016-808, 2016
Manuscript under review for journal Atmos. Chem. Phys.
Published: 5 October 2016

Atmospheric Chemistry and Physics Discussions

Figure 6. Convective core fraction density function for single (red) and multi (blue) core systems.

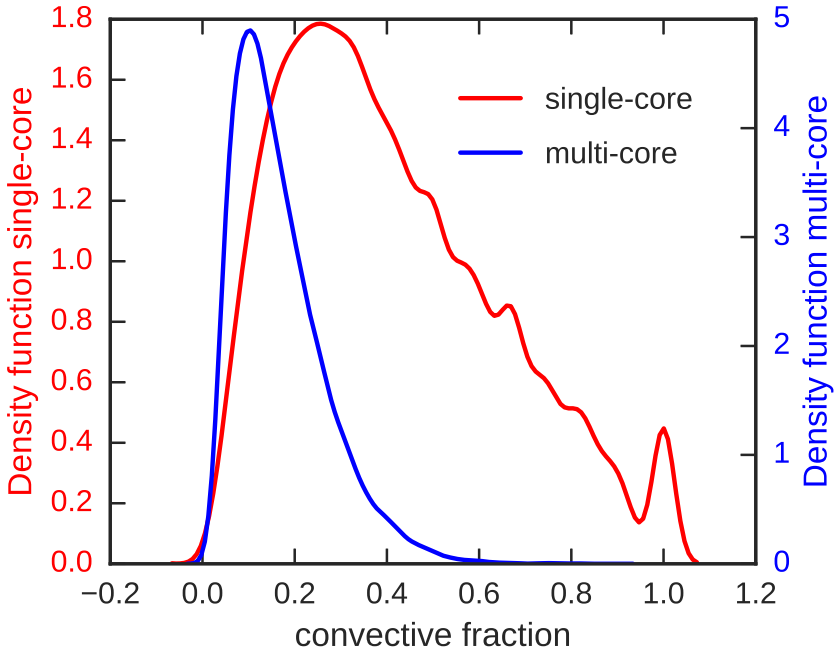

Atmos. Chem. Phys. Discuss., doi:10.5194/acp-2016-808, 2016
Manuscript under review for journal Atmos. Chem. Phys.
Published: 5 October 2016

Atmospheric Chemistry and Physics Discussions

Figure 7. Physical properties of single-core convective systems for eleven maturity steps defined by fraction of convective area, separately over ocean and over land and during night (AM) and early afternoon (PM): a) cloud system size, b) convective core size, c) thin cirrus over cirrus area, d) cloud system average emissivity, e) minimum temperature within convective core, f) average convective core rain rate.

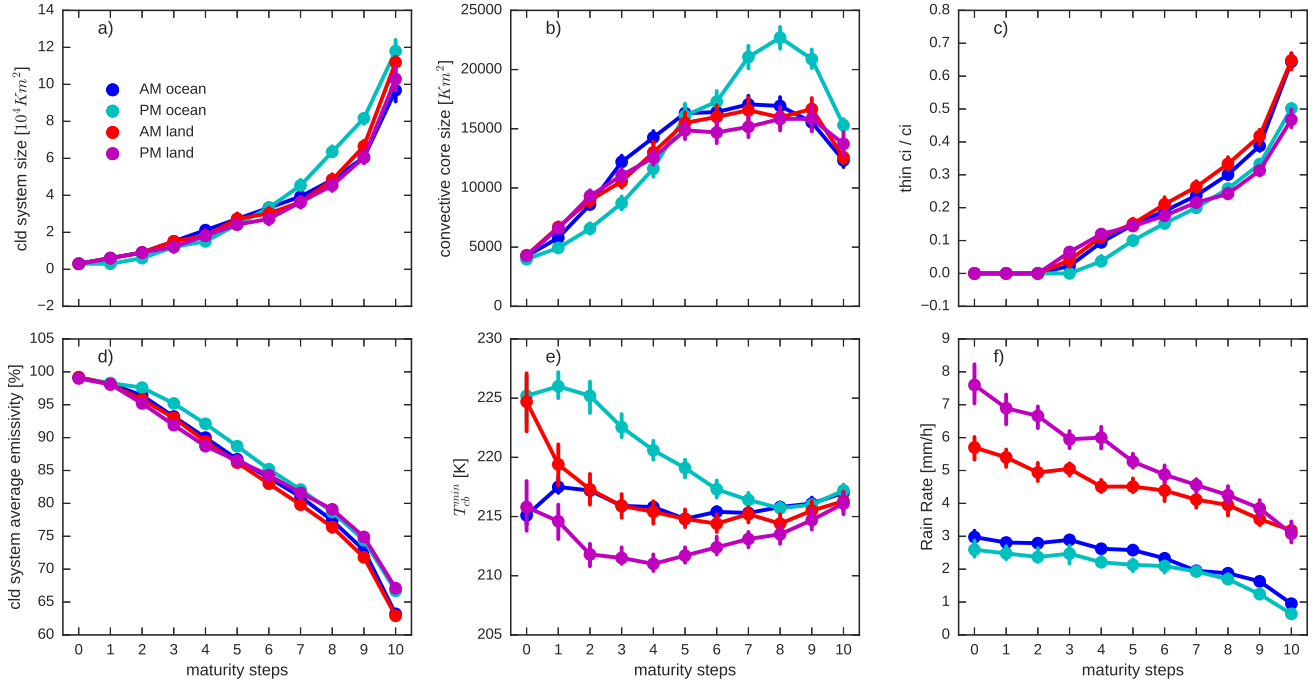

Atmos. Chem. Phys. Discuss., doi:10.5194/acp-2016-808, 2016
Manuscript under review for journal Atmos. Chem. Phys.
Published: 5 October 2016

Atmospheric Chemistry and Physics Discussions

Figure 8. Number of cloud systems in each maturity step, separately over ocean and over land and during night (AM) and early afternoon (PM).

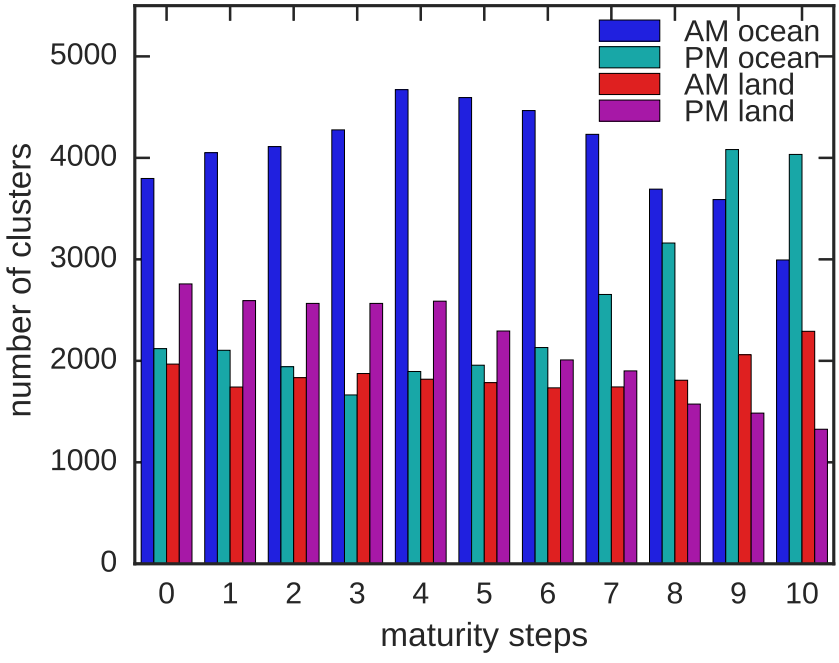

Atmos. Chem. Phys. Discuss., doi:10.5194/acp-2016-808, 2016
Manuscript under review for journal Atmos. Chem. Phys.
Published: 5 October 2016

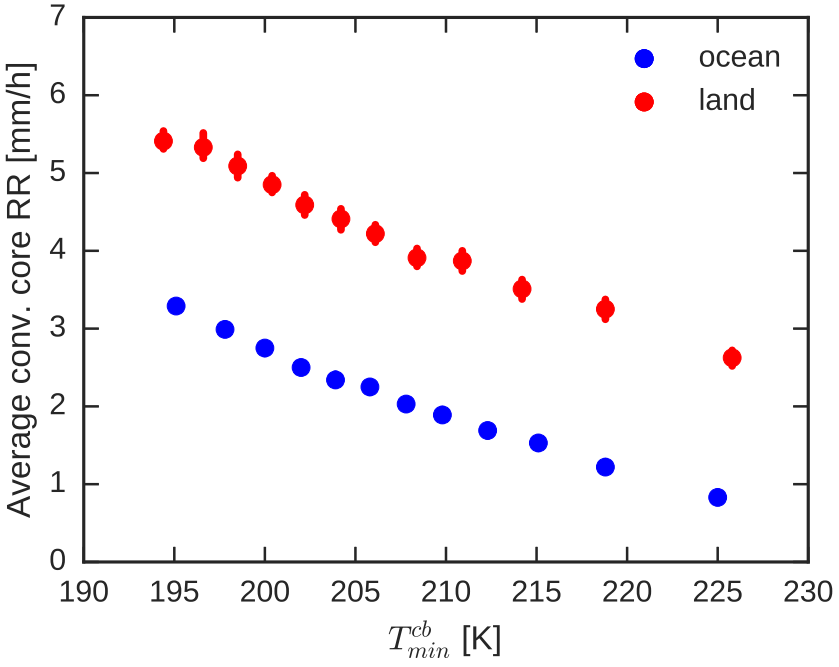

Figure 9. Rain rate of convective core as a function of minimum temperature within the convective core, separately over land (red) and ocean (blue).

Atmos. Chem. Phys. Discuss., doi:10.5194/acp-2016-808, 2016
Manuscript under review for journal Atmos. Chem. Phys.
Published: 5 October 2016

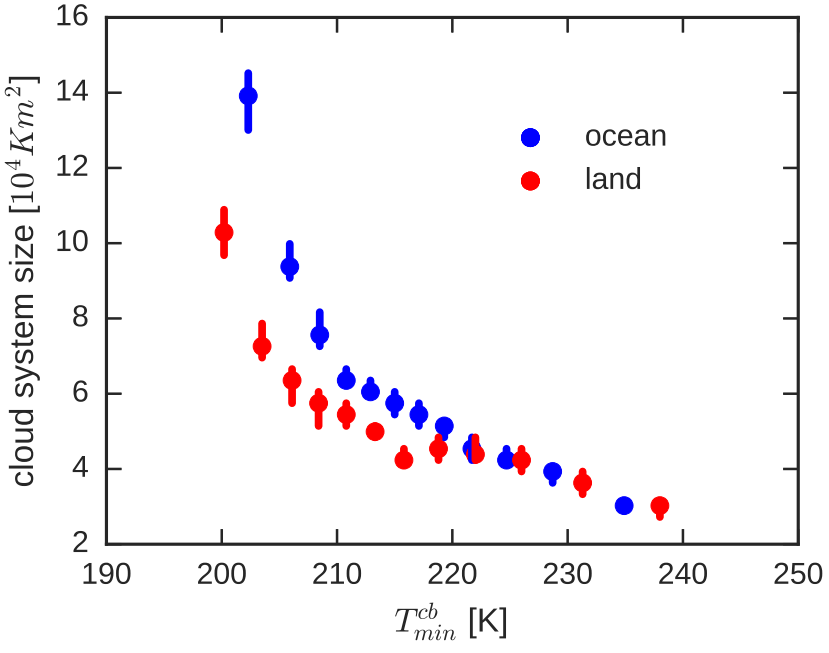

Figure 10. Single-core system horizontal extent versus minimum temperature within convective core, separately over land (red) and ocean (blue).

Atmos. Chem. Phys. Discuss., doi:10.5194/acp-2016-808, 2016
Manuscript under review for journal Atmos. Chem. Phys.
Published: 5 October 2016

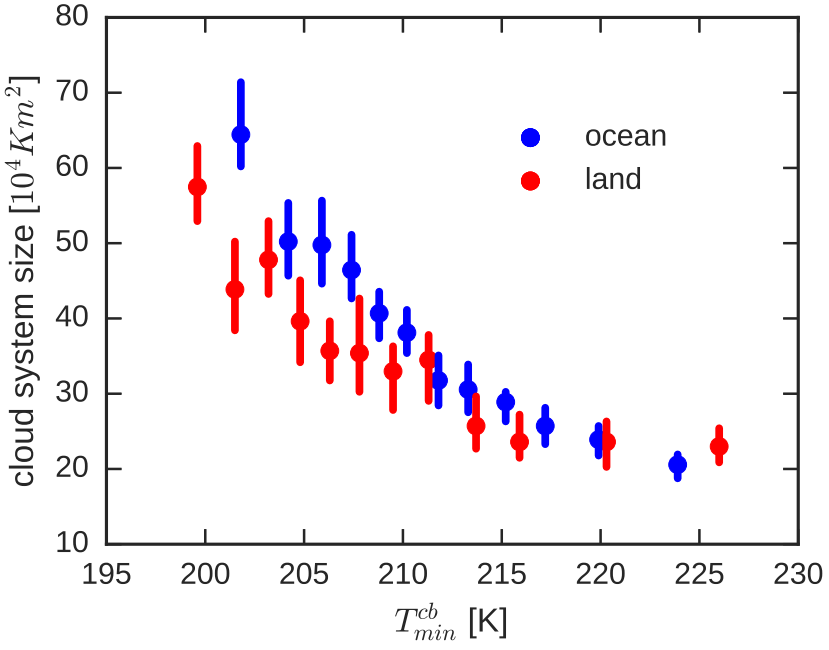

Figure 11. Multi-core system horizontal extent versus average of minimal temperature within convective cores, separately over land (red) and ocean (blue).

Atmos. Chem. Phys. Discuss., doi:10.5194/acp-2016-808, 2016
Manuscript under review for journal Atmos. Chem. Phys.
Published: 5 October 2016

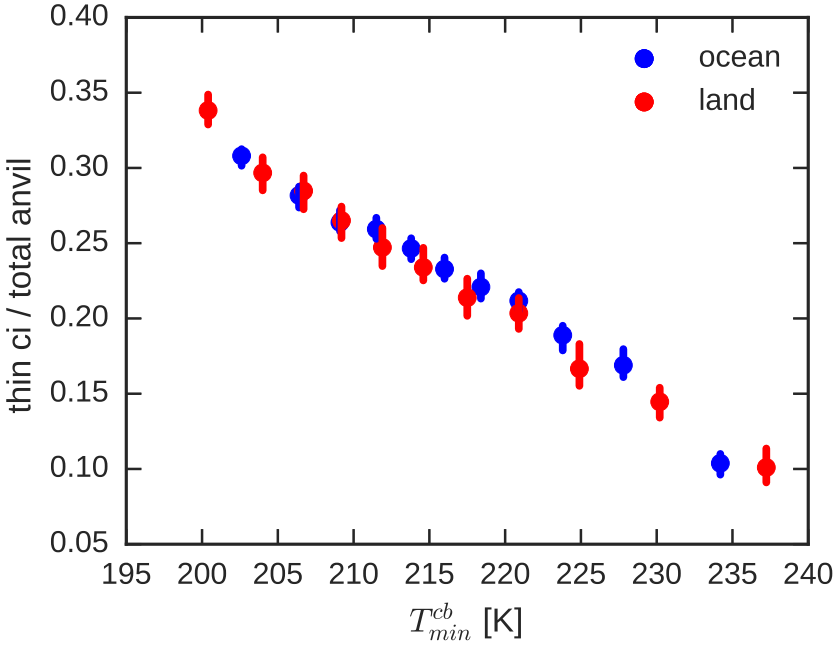

Figure 12. Thin cirrus over total anvil area as a function of minimum temperature within convective core for single-core systems, separately over land (red) and ocean (blue).

Atmos. Chem. Phys. Discuss., doi:10.5194/acp-2016-808, 2016
Manuscript under review for journal Atmos. Chem. Phys.
Published: 5 October 2016

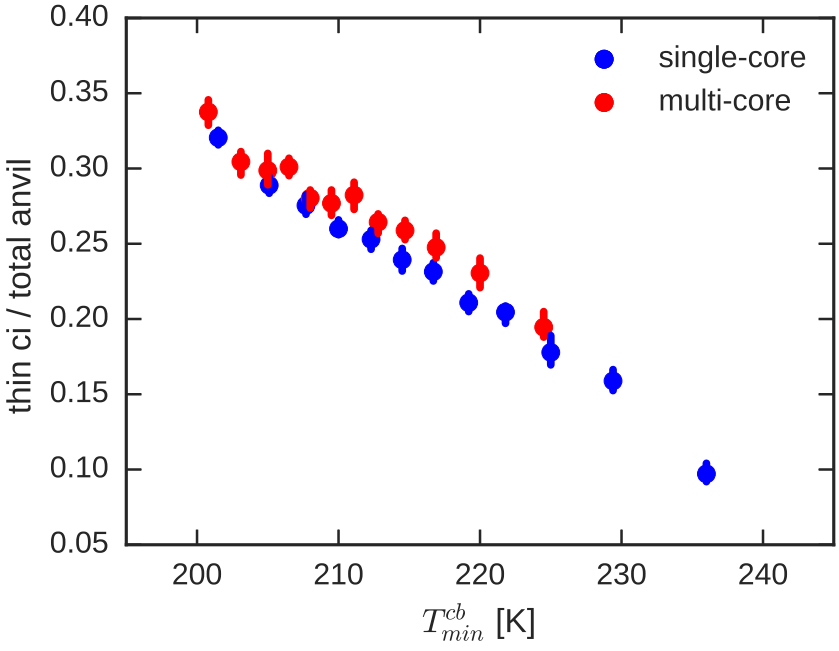

Figure 13. Thin cirrus over total anvil area as a function of minimum temperature within convective core(s), separately for single-core (blue) and multi-core (red) systems.

Atmos. Chem. Phys. Discuss., doi:10.5194/acp-2016-808, 2016
Manuscript under review for journal Atmos. Chem. Phys.
Published: 5 October 2016

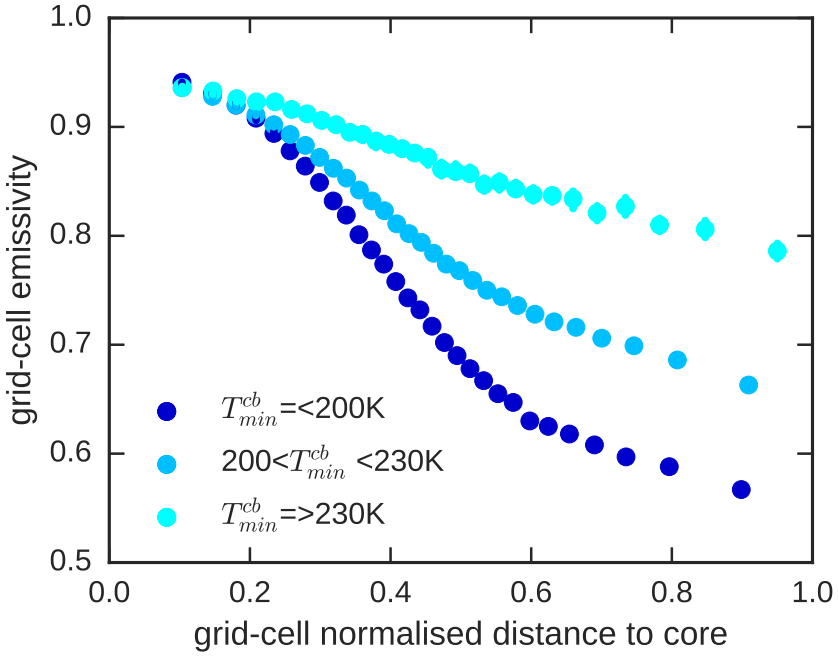

Figure 14. Emissivity within cloud system as a function of the normalized distance to the convective core. Single-core system are considered for three classes of convective intensity represented by intervals in T^{cb}_{min}.

Atmos. Chem. Phys. Discuss., doi:10.5194/acp-2016-808, 2016
Manuscript under review for journal Atmos. Chem. Phys.
Published: 5 October 2016

Atmospheric Chemistry and Physics Discussions

	isolated cirrus	single core	multi-core
Numb.of systems	>95%	3%	1%
Coverage	25%	10%	65%
Median size	10^4Km^2	10*10^4 Km^2	200*10^4 Km^2

Table 1. Fraction of occurrence, coverage and median size for isolated cirrus systems, systems with one convective core and with multiple convective cores, over the latitude band 30° N-30° S, annual average over the period 2003-2015.